Fermi National Accelerator Laboratory

FERMILAB-Conf-94/020

Synchro-Betatron Effects in Hadron Machines

King-Yuen Ng

Fermi National Accelerator Laboratory
P.O. Box 500, Batavia, Illinois 60510

January 1994

Presented at the *6th Advanced ICFA Beam Dynamics Workshop*, Funchal, Portugal, October 25-30, 1993

Operated by Universities Research Association Inc. under Contract No. DE-AC02-76CHO3000 with the United States Department of Energy

SYNCHRO-BETATRON EFFECTS IN HADRON MACHINES

King-Yuen Ng

Fermi National Accelerator Laboratory, P.O. Box 500, Batavia, IL 60510*

I. SYNCHRO-BETATRON RESONANCES

In electron machines, there are strong synchrotron radiation and random excitations, and high rf voltage is necessary to compensate for the energy loss. The synchrotron tune is therefore rather large and is of the order of $\nu_s \sim 0.1$. In proton machines, however, synchrotron radiation is negligibly small, and the rf voltage is therefore much smaller. Typically, we have $\nu_s \sim 0.001$ for big rings like the Fermilab Main Ring, Tevatron, and the SSC. For this reason, synchro-betatron coupling resonance (SBR) does not occur in big proton rings.

Exceptions are smaller rapid-cycling proton boosters, where high rf voltage is necessary. The Fermilab Booster has a cycling rate of 15 Hz, with an rf voltage that can be ramped to ~ 0.8 MV. With an injection energy of 200 MeV, the synchrotron tune can reach a maximum of $\nu_s \sim 0.075$ in less than 2 msec. The space-charge tune shift is ~ 0.3. In order to avoid the half-integer resonance, the *bare* betatron tunes are usually pushed up to $\nu_\beta = 6.8$ or 6.9. It was reported that the Booster cannot operate with ν_β up to 6.95. It is possible that SBR occurs in this regime.

II. SYNCHRO-BETATRON EFFECTS

Besides SBR, there are also other synchro-betatron effects. For example, the small and slow synchrotron oscillations can serve as a modulation to the betatron motion, and lead to transverse and/or longitudinal emittance growth. This is similar to the perturbation by noise and current ripple when there is nonzero dispersion at the rf.

An experiment was performed at the Tevatron, [1] where random noise was added to the rf phase at the betatron sideband frequency f_b, and the horizontal emittance growth rate r was measured. The bunch had an energy E, revolution frequency f_0, in a bucket with rf voltage V. Theoretically, the growth rate is

$$r = \frac{f_0^2 H}{8\Delta f_0}\left(\frac{eV}{E}\right)^2 \left|\tilde{\phi}(f_b)\right|^2 , \tag{2.1}$$

where

$$H = \frac{1}{\beta}\left|D^2 + (\beta D' - \tfrac{1}{2}\beta' D)^2\right| . \tag{2.2}$$

In the above, $\tilde{\phi}(f_b)$ is the Fourier transform of the perturbing rf phase integrated over the frequency bin Δf_0 at the betatron sideband, whereas β, D, β', and D' are the betatron function, dispersion function and their derivatives at the rf. For the Tevatron, $H \sim 0.090 \pm 0.020$ m. The experimental result is plotted in Fig. 1 with the growth rate of $r = (3.3 \pm 0.7) \times 10^{-7}|\tilde{\phi}|^2$ m-rad/sec, while the theoretical rate is $r = (4.3 \pm 0.9) \times 10^{-7}|\tilde{\phi}|^2$ m-rad/sec.

*Operated by the Universities Research Association, Inc., under contract with the U.S. Department of Energy.

III. GROUND MOTION

Ground movements of the quadrupoles and current ripples in the dipoles will couple to the longitudinal phase space and lead to emittance growth. Since the synchrotron frequency of the SSC would have been $f_s \sim 3$ to 4 Hz, the effect of ground motion to the SSC can be very significant.

An experiment was performed at IUCF by modulating a Panofsky dipole and monitoring the longitudinal phase space. [2] The modulation gives an island system of order one in the longitudinal phase space, and the bunch area will be increased.

The most important sources of ground motion at the SSC site are a train passing 20 m above the tunnel and some quarry blasts 9 miles away. The conclusion drawn by the experiment is: the train passing may increase the bunch area by $\sim 80\%$, and the quarry blast by 200%. These increases are finite, because the spectra of these perturbations peak sharply at some frequencies. For a source of random movement, the growths will be unbounded.

IV. CURRENT RIPPLE

Current ripple in the dipoles will produce betatron motion and will be coupled to the longitudinal phase space if the dispersion at the dipoles is nonzero.

When the synchrotron frequency is ramped upward through the frequency of the current ripple at $f_m = 60$ Hz, the island of order one in the longitudinal phase space discussed in the previous section will move outward. If the ramping rate is small enough, there will be adiabatic trapping and particles will move even outside the bucket, as shown by the simulation in Fig. 2. The condition for this to occur is [3]

$$\Delta\nu_s < \frac{3\pi}{8} a^{4/3} \nu_m \ , \tag{4.1}$$

where $\Delta\nu_s$ is the increase of the synchrotron tune per turn, ν_m is the tune of the perturbation, and a is the driving amplitude.

For the Relativistic Heavy Ion Collider (RHIC), the ramp rate is $\Delta\nu_s = 2.45 \times 10^{-9}$ per turn in the vicinity of $f_s = 60$ Hz. Adiabatic trapping will occur when the current ripple is as high as $\epsilon = 2 \times 10^{-5}$. A modification of the design has been made.

V. PHASE DIAGRAM AND CHAOS

The transverse phase space is always modulated by synchrotron oscillation or some other oscillations. It is important to study the modulated phase space.

When a resonance frequency Q_I is modulated by $q \sin 2\pi n Q_m$, where n is the turn number, the effects of the modulation can be plotted as different phases in the q-Q_m space. Such a plot was illustrated by Peggs [4] in Fig. 3. The boundary between the regions of *strong sidebands* and *chaos* is the condition of overlapping sideband islands, while the other boundaries are given by the validity of the small-angle driven pendulum solution. However, recently Zimmerman [5] suggested a different criterion for the boundary of the chaotic region by taking into account the thickness of the stochastic layer near the separatrices. His q-Q_m phase diagram is illustrated in Fig. 4, where the dotted curves are the suggested chaotic boundary. There are important differences between Figs. 3 and 4. Figure 3 shows that the region where $Q_m \sim Q_I$ is highly chaotic no matter how small the modulation amplitude q is. It also predicts a stable region of strong sideband. This is obviously not so in Fig. 4. Zimmerman performed a simple octupole-kick-map with result of stability shown as open circles and stochasticity as solid circles in Fig. 4, which confirm his chaotic criterion. On the other hand, there are in Fig. 3 also the simulation results of Satogata, [6] where he tracked for the disappearance of the stable fixed points of the island chain. The simulations do conform to the partitions of Fig. 3.

We therefore have a contradiction: Which chaotic criterion is correct? For this we need to answer first the question: What is chaos? Peggs defined it as the disappearance of stable fixed point, while Zimmerman's definition corresponds to *global chaos*, when the chaotic regions are all connected. Recently Lee *et al.* [7] studied a modulated double rf cavity system. The central region of the longitudinal phase space should be in chaos, because of the overlapping of infinitely many higher-order island chains. A simulation is shown in Fig. 5 with the central region magnified. We definitely see that this region is in chaos, although there are still isolated islands with stable flow trajectories. This is a situation of *global chaos* but not the type of chaos defined by Peggs. In other words, Peggs' definition seems to be more stringent. However, this still cannot answer why there is chaos in Peggs' case when $Q_m \sim Q_I$ even at small modulated amplitude but not in Zimmerman's case. Further understanding is necessary.

VI. EXTRACTION

Resonances need not be bad. For example, the half-integer and third-integer resonances have been successfully used for beam extraction. Peggs *et al.* [8] demonstrated that the SBR can be used to transport beam to a crystal for crystal channeling extraction.

References

[1] S.R. Mane and G. Jackson, Nucl. Inst. Meth. **A276**, 8 (1989).

[2] M. Syphers, *et al.*, Phys. Rev. Lett. **71**, 719 (1993).

[3] K.Y. Ng, these proceedings.

[4] T. Chen and S. Peggs, Proceedings of the third ICFA Beam Dynamics Workshop, Novosibirsk, 1989.

[5] F. Zimmermann, Thesis, DESY 93-059, May 1993.

[6] T. Satogata, Thesis, 1992.

[7] S.Y. Lee, *et al.*, 1993, submitted to Phys. Rev. Lett.

[8] S. Peggs, *et al.*, these proceedings.

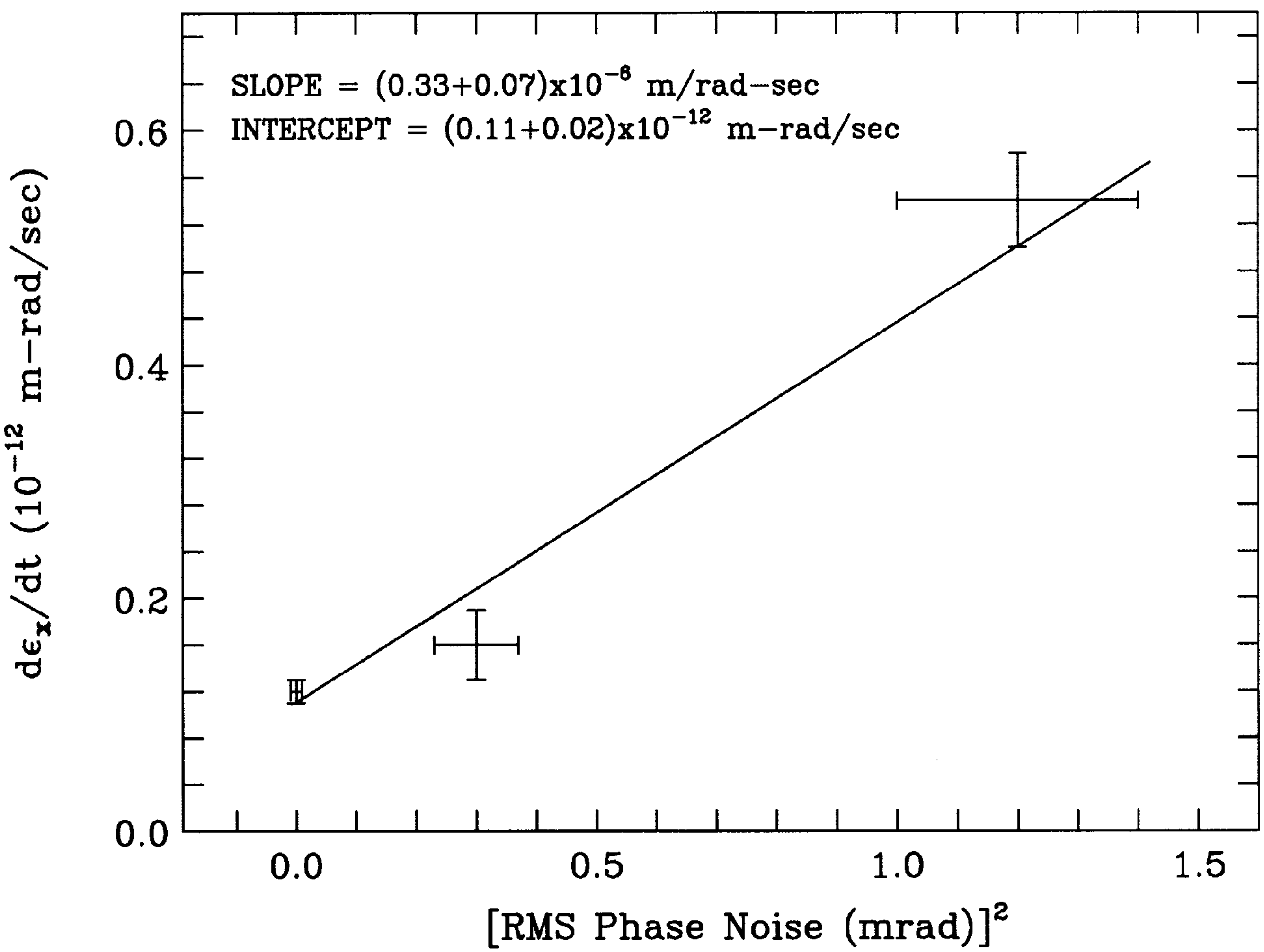

Figure 1: Rate of growth of horizontal emittance as a function of rms phase noise.

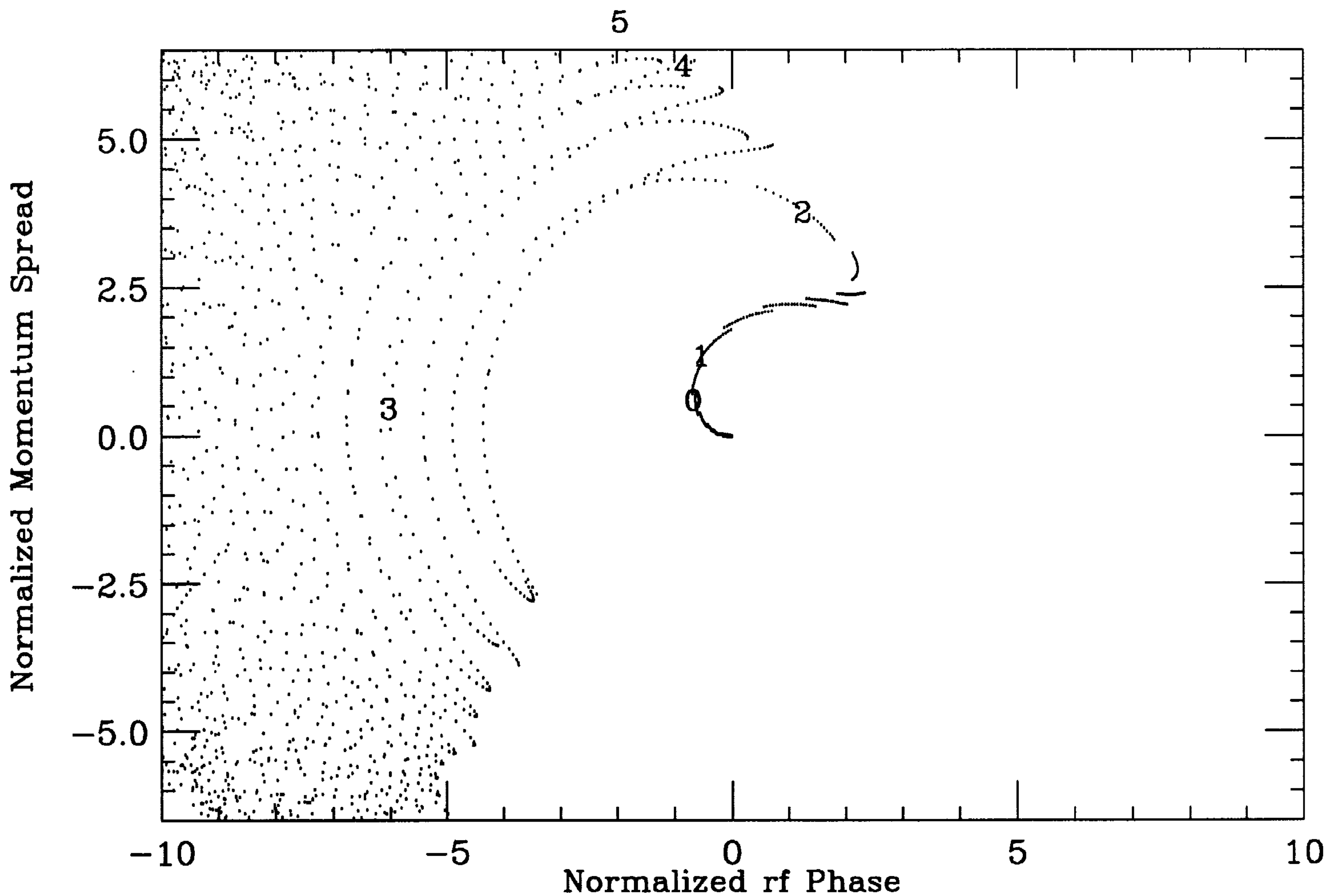

Figure 2: Adiabatic trapping of a bunch particle due to current ripple at 60 Hz.

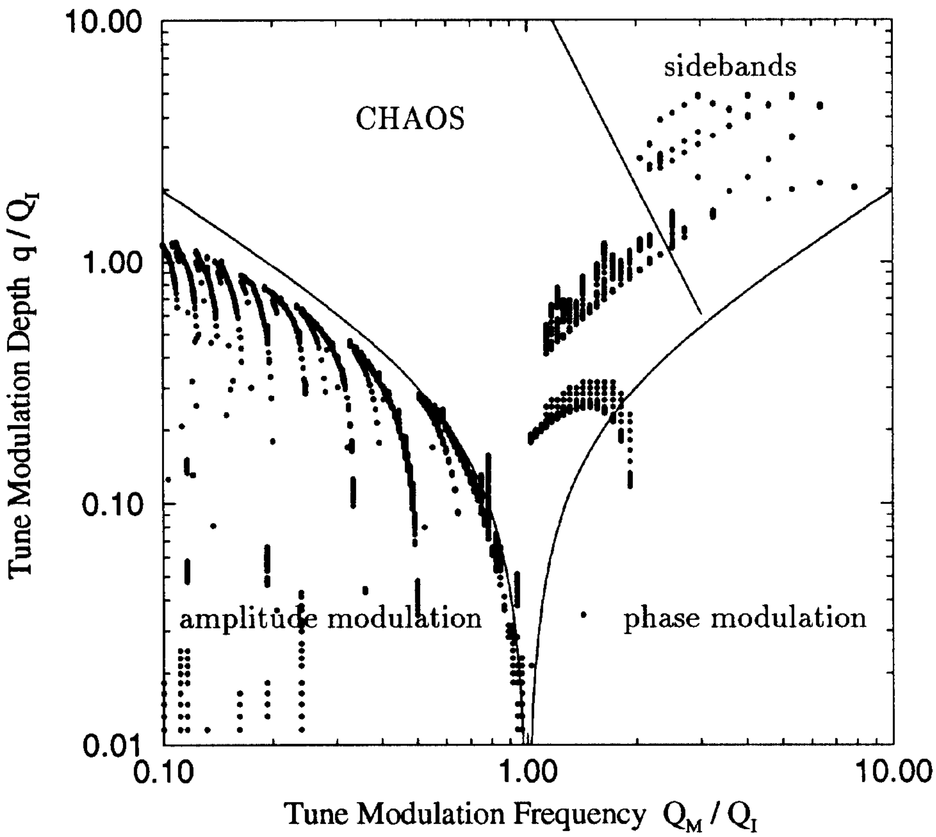

Figure 3: Plot of modulation amplitude versus modulation frequency. The partition of the q-Q_m space is given by Peggs. [4] The points are simulation results of Satogata [6] for the disappearance of the stable island fixed point.

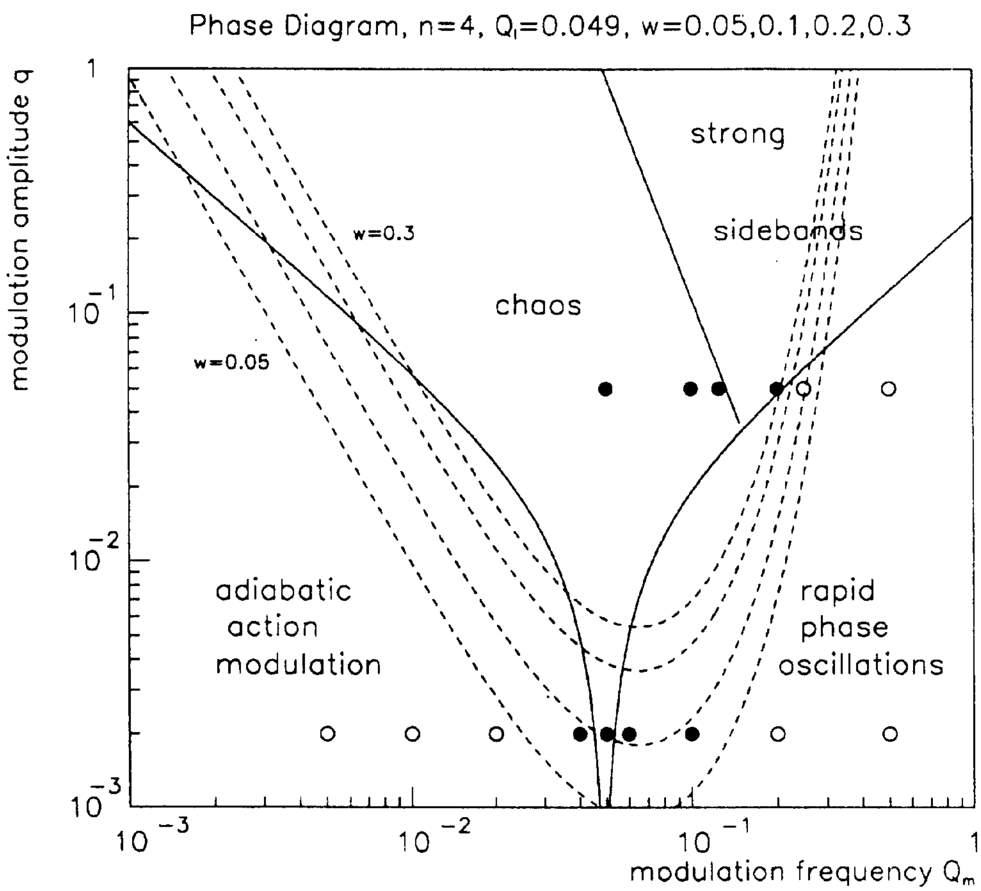

Figure 4: Plot of modulation amplitude versus modulation frequency. The dotted curves are the boundary of the chaotic region given by Zimmerman, [5] whose simulation results are denoted by black (chaotic) and open (nonchaotic) circles.

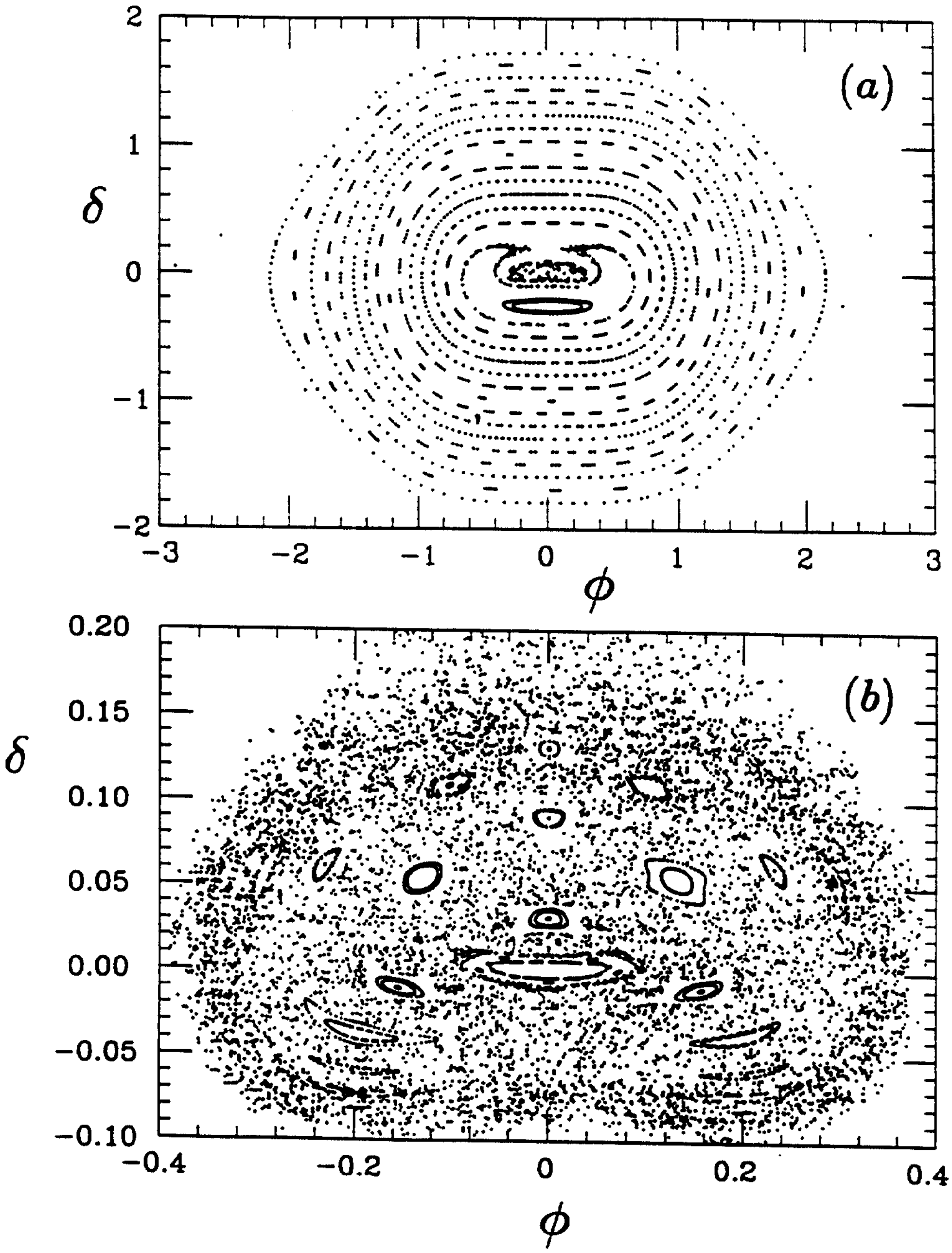

Figure 5: (a) Plot of the longitudinal phase space for a double rf system. At the center of the phase space magnified in the lower plot (b), isolated stable islands are seen in the sea of global chaos.